Proposal for a Bell test in cavity optomagnonics

Hong Xie,[1,*] Zhi-Gao Shi,[1] Le-Wei He,[1] Xiang Chen,[2,3,4] Chang-Geng Liao,[5] and Xiu-Min Lin[2,3,4,†]

[1]*Department of Mathematics and Physics, Fujian Jiangxia University, Fuzhou 350108, China*

[2]*Fujian Provincial Key Laboratory of Quantum Manipulation and New Energy Materials, College of Physics and Energy, Fujian Normal University, Fuzhou 350117, China*

[3]*Fujian Provincial Engineering Technology Research Center of Solar Energy Conversion and Energy Storage, Fuzhou 350117, China*

[4]*Fujian Provincial Collaborative Innovation Center for Advanced High-Field Superconducting Materials and Engineering, Fuzhou 350117, China*

[5]*School of Information and Electronic Engineering (Sussex Artificial Intelligence Institute), Zhejiang Gongshang University, Hangzhou 310018, China*

(Received 3 May 2021; revised 14 October 2021; accepted 24 January 2022; published 1 February 2022)

We present a proposal to test the Bell inequality in the emerging field of cavity optomagnonics, where a sphere of ferromagnetic crystal supports two optical whispering gallery modes and one magnon mode. The two optical modes are driven by two laser pulses, respectively. Entanglement between the magnon mode and one of the two optical modes will be generated by the first pulse, and the state of the magnon mode is subsequently mapped into another optical mode via the second pulse. Hence correlated photon-photon pairs are created out of the cavity. A Bell test can be implemented by using these pairs, which enables us to test the local hidden-variable models at macroscopic scales. Our results show that a significant violation of the Bell inequality can be obtained in the weak-coupling regime. The violation of the Bell inequality not only verifies the entanglement between magnons and photons, but also implies that cavity optomagnonics is a promising platform for quantum information processing tasks.

DOI: 10.1103/PhysRevA.105.023701

I. INTRODUCTION

A hybrid system enables the combination of distinct physical systems with complementary characteristics, which has played an important role in the development of quantum information [1–3] and quantum sensing [4]. In recent years, a new hybrid system based on the collective magnetic excitations in magnetic materials has emerged as a platform for novel quantum technologies [5,6]. The quanta of the collective magnetic excitations, called magnons, have great tunability and a low damping rate which make them ideal information carriers. The magnons can interact coherently with microwave photons via magnetic dipole interaction [7], and the strong coupling between magnons and microwave photons has been demonstrated experimentally with a magnetic insulator yttrium iron garnet (YIG) sphere [8–12] and stripe [13,14]. This coupling not only allows us to study magnon-photon entanglement [15,16], but also makes it possible to engineer an effective interaction between magnons and superconducting qubits [17,18]. Benefiting from the large spin density of a YIG crystal, magnons in a YIG sphere can also couple with phonons through magnetostrictive interaction [19,20]. More recently, an exciting field named cavity optomagnonics has emerged, in which a YIG sphere supports both the whispering gallery modes (WGMs) for optical photons and magnetostatic modes for magnons [21].

Different from the resonance interaction between microwave photons and magnons, the optomagnonic coupling between optical photons and magnons is parametrical. This is because the frequency of optical photons is in the range of 100 THz, while the magnons are in the gigahertz range. Indeed, the optomagnonic coupling originates from magneto-optical effects, which have been used to study magnon-based microwave-optical information interconversion [22]. By cavity-enhanced magnon-photon coupling in cavity optomagnonical systems, several experiments have demonstrated magnon-induced Brillouin light scattering of the optical WGMs [23–27]. These experiments work in the weak-coupling regime, where the intrinsic optomagnonic coupling strength is much lower than the decay rates of both optical photons and magnons. A theoretical framework for cavity optomagnonics has been established to overcome the shortcoming in this field [28–35]. It is expected that the strong optomagnonic coupling will be achieved in the future, opening the opportunity for applications such as optical cooling the magnons [36], preparation of a magnon Fock state [37], magnon-based photon blockade [38], and a magnon cat state [39,40].

Although it is still a challenge to realize the quantum features of cavity optomagnonics in the weak-coupling regime, it is interesting to determine whether the nonclassicality can be characterized without quantum assumptions. A Bell test is a genuine test of nonclassicality without the need of

*xh@fjjxu.edu.cn
†xmlin@fjnu.edu.cn

quantum formalism [41]. In this paper, we propose to violate the Clauser-Horne-Shimony-Holt (CHSH) inequality (a Bell-type inequality) [42] by using entanglement between optical photons and magnons in a YIG sphere, which allows us to test the local hidden-variable models at macroscopic scales. A test of the CHSH inequality has been performed in various systems [43–52], including recently in a macroscopic optomechanical system [53–55]. However, it would be interesting to perform a Bell test in a magnetically ordered solid-state system consisting of millions of spins.

The model of our proposal involves two nondegenerate cavity modes and one magnon mode, which has been demonstrated with YIG spheres in recent experiments [23–27]. Starting with a cavity optomagnonical system close to its ground state, we use two laser pulses to excite the two cavity modes, respectively. First, optical mode 2 is driven at resonance and then the entanglement between the magnon mode and optical mode 1 can be obtained by means of a two-mode squeezed interaction. The magnonic state can be subsequently mapped into the photonic state of optical mode 2 by a beam-splitter interaction, which is induced by driving optical mode 1 with the second pulse. Therefore, the photon-photon pairs of the two optical modes are generated out of the cavity optomagnonical system. The correlation of the photon-photon pairs is measured by a photon detector preceded by a displacement operation in phase space. Our results show that a significant violation of the CHSH inequality can be obtained in the experimentally relevant weak-coupling regime. The violation of the CHSH inequality rules out any local and realistic explanation of the measured data without quantum assumption and it also verifies the existence of entanglement between magnons and photons.

The paper is organized as follows. The model based on cavity optomagnonics is presented in Sec. II. Section III provides analytical discussion of the dynamical evolution of the system and the violation of the CHSH inequality in phase space. Section IV discusses the results and provides a summary.

II. MODEL

Consider a cavity optomagnonical system where a YIG sphere supports both the WGMs for optical photons and magnetostatic modes for magnons. The optomagnonic Hamiltonian is given by

$$H = H_0 + H_{\rm int} + H_{\rm dr}, \tag{1}$$

where

$$H_0 = \omega_1 a_1^\dagger a_1 + \omega_2 a_2^\dagger a_2 + \omega_m m^\dagger m \tag{2}$$

is the free-evolution part of the system with bosonic operators a_i $(i = 1, 2)$ and m, and ω_i and ω_m are the frequencies of the cavity modes and the magnon mode, respectively. The Hamiltonian $H_{\rm int}$ describes the interaction between two nondegenerate cavity modes and the magnon mode, which can be written as

$$H_{\rm int} = g(a_1 a_2^\dagger m + a_1^\dagger a_2 m^\dagger). \tag{3}$$

Note that such an interaction in the optomagnonical system is subject to selection rules of angular momentum and the energy conservation requirement with $\omega_2 - \omega_1 = \omega_m$ [25,30,32]. This means that the creation (annihilation) of a photon in optical mode 2 is accompanied by the annihilation (creation) of a photon in optical mode 1 and a magnon. This optomagnonic coupling has been demonstrated experimentally in a YIG sphere, where the transverse-electric modes and the transverse-magnetic modes of the cavity interact with the magnetostatic modes [23–27]. When the cavity is pumped with an external field, the driving Hamiltonian reads

$$H_{\rm dr} = \epsilon_i (a_i e^{i\omega_L t} + a_i^\dagger e^{-i\omega_L t}), \tag{4}$$

where $i = 1$ or 2 and ϵ_i and ω_L are the driving amplitudes and the driving frequencies, respectively. In the rotating frame of the driving field, the full Hamiltonian of the system becomes

$$\begin{aligned} H =\ & \Delta_1 a_1^\dagger a_1 + \Delta_2 a_2^\dagger a_2 + \omega_m m^\dagger m \\ & + g(a_1 a_2^\dagger m + a_1^\dagger a_2 m^\dagger) + \epsilon_i (a_i + a_i^\dagger), \end{aligned} \tag{5}$$

with $\Delta_i = \omega_i - \omega_L$.

In the case in which cavity mode 2 is pumped and cavity mode 1 is undriven, following the standard linearization procedure, we split both the cavity modes and the magnon mode into an average amplitude and a fluctuation term, i.e., $a_i \to \alpha_i + a_i$ and $m \to \beta + m$. The average amplitude can be obtained as $\alpha_2 = \epsilon_2/(i\kappa_{2,\rm ex}/2 - \Delta_2)$ and $\beta = 0$, where $\kappa_{i,\rm ex}$ denotes the loss rate of the ith cavity mode associated with the external coupling. Since only mode 2 is pumped we have $\alpha_1 = 0$. Note that the coherent amplitude α_i can be chosen to be real by a suitable choice of the phase of the pumping field. The linearized Hamiltonian of the system in the interaction picture can be gained

$$H_{\rm int1} = G_1 (a_1 m e^{i(\Delta_1 + \omega_m)t} + a_1^\dagger m^\dagger e^{-i(\Delta_1 + \omega_m)t}), \tag{6}$$

where $G_1 = g\alpha_2$ and the small nonlinear term has been neglected. When cavity mode 2 is driven at resonance $\omega_L = \omega_2$ such that $\Delta_1 = -\omega_m$, Eq. (6) becomes

$$H_{\rm int1} = G_1 (a_1 m + a_1^\dagger m^\dagger), \tag{7}$$

which represents a two-mode squeezing interaction. Assuming that both the optical modes and the magnon mode are initially prepared in their ground state, the entanglement between cavity mode 1 and the magnon mode can be generated after the pulse duration. In the weak-coupling regime, i.e., when the effective optomagnonic coupling strength G_1 is much lower than the decay rate κ_1 of the cavity, the entangled photons leak out of the cavity faster than they are generated, and thus the magnon mode becomes entangled with a traveling optical pulse. Here we will show the entangled states of the traveling-wave optical fields and the magnon mode can be utilized to test the Bell inequality.

To perform a measurement on the magnon mode, the magnon state should be transferred to the optical field. We now consider that only cavity mode 1 is pumped. Similar to the process of pumping mode 2 discussed above, we can obtain the interaction Hamiltonian

$$H_{\rm int2} = G_2 (a_2 m^\dagger e^{-i(\Delta_2 - \omega_m)t} + a_2^\dagger m e^{i(\Delta_2 - \omega_m)t}), \tag{8}$$

with $G_2 = g\alpha_1$, and the average amplitude of mode 1 is given by $\alpha_1 = \epsilon_1/(i\kappa_{1,\rm ex}/2 - \Delta_1)$. When mode 1 is driven at resonance $\omega_L = \omega_1$ so that $\Delta_2 = \omega_m$, the Hamiltonian becomes

$$H_{\rm int2} = G_2 (a_2 m^\dagger + a_2^\dagger m). \tag{9}$$

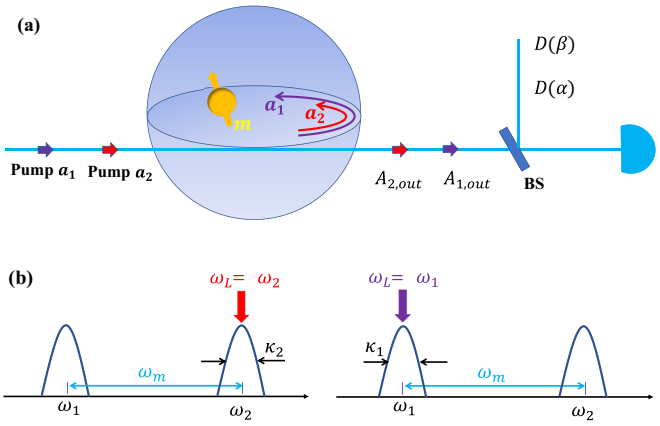

FIG. 1. (a) Schematic of the cavity optomagnonical system for the Bell test proposal. The first pumping pulse drives cavity mode 2 at resonance to create entanglement between cavity mode 1 and magnon mode m. The second pulse drives cavity mode 1 at resonance to transfer the state of the magnon mode to cavity mode 2. The photons of cavity modes 1 and 2 leaking out of the cavity ($A_{1,\mathrm{out}}$ and $A_{2,\mathrm{out}}$) are measured with a photon detector preceded by a displacement, which can be realized by an input coherent state and beam splitter (BS). (b) Two nondegenerate cavity modes a_1 and a_2 are detuned by a magnon resonance frequency ω_m.

The Hamiltonian is often referred to as a beam-splitter interaction, which is relevant for the state transfer between cavity mode 2 and the magnon mode.

Note that the coupling between cavity mode 1 (2) and the magnon mode is achieved by pumping the other cavity mode 2 (1). The proposal for a Bell test in cavity optomagnonics is depicted in Fig. 1. It can be summarized as three steps. (i) The entanglement between cavity mode 1 and the magnon mode is generated by resonantly pumping mode 2. (ii) The quantum state of the magnon mode is subsequently mapped into cavity mode 2 by resonantly driving mode 1, and therefore modes 1 and 2 are entangled. (iii) The measurement for the correlation between the two traveling optical pulses of modes 1 and 2 is performed. The measurement setting consists of a single-photon detector preceded by a displacement operation $D(\alpha)$, which can be implemented by an input coherent state and an unbalanced beam splitter [56]. Such a measuring apparatus has been used for Bell tests in optical experiments [57].

III. BELL TEST IN CAVITY OPTOMAGNONICS

A. Generation of optomagnonical entanglement

In this section we study the evolution of the dynamics of the system and the generation of optomagnonical entanglement for the Bell test. When cavity mode 2 is driven at resonance, the quantum Langevin equations with the Hamiltonian H_{int1} are

$$\frac{da_1}{dt} = -iG_1 m^\dagger - \frac{\kappa_1}{2}a_1 + \sqrt{\kappa_{1,\mathrm{ex}}}a_{1,\mathrm{in}} + \sqrt{\kappa_{1,\mathrm{i}}}a_{1,\mathrm{th}}, \quad (10a)$$

$$\frac{dm}{dt} = -iG_1 a_1^\dagger - \frac{\gamma}{2}m + \sqrt{\gamma}m_{\mathrm{in}}, \quad (10b)$$

where $\kappa_1 = \kappa_{1,\mathrm{ex}} + \kappa_{1,\mathrm{i}}$ is the total linewidth of cavity mode 1 in terms of the external coupling $\kappa_{1,\mathrm{ex}}$ and material optical loss $\kappa_{1,\mathrm{i}}$, γ denotes the decay rate of the magnon mode, $a_{1,\mathrm{in}}$ is the vacuum input noise for the cavity, $a_{1,\mathrm{th}}$ denotes the thermal noise introduced by material, and m_{in} represents the stochastic magnetic field. The noise correlators associated with the memoryless Markov-like fluctuations are $\langle X^\dagger(t)X(t')\rangle = \bar{n}_{\mathrm{th}}\delta(t-t')$ and $\langle X(t)X^\dagger(t')\rangle = (\bar{n}_{\mathrm{th}}+1)\delta(t-t')$, where $X \in \{a_{1,\mathrm{in}}, a_{1,\mathrm{th}}, m_{\mathrm{in}}\}$. The optical field has zero thermal occupation ($\bar{n}_{\mathrm{th}} \approx 0$) even at room temperature, but this is not the case for magnons.

For simplicity, we consider the total loss of the cavity to be dominated by the external coupling $\kappa_1 \approx \kappa_{1,\mathrm{ex}} \gg \kappa_{1,\mathrm{i}}$, i.e., the cavity is overcoupled. Assuming that the magnon is initially prepared in its ground state, then the noise introduced by material is negligibly small. After neglecting the decay of the magnon mode, which is reasonable when the pulse duration is shorter than the magnon decoherence time $(\gamma\bar{n}_{\mathrm{th}})^{-1}$, the quantum Langevin equations can be simplified as

$$\frac{da_1}{dt} \approx -iG_1 m^\dagger - \frac{\kappa_1}{2}a_1 + \sqrt{\kappa_1}a_{1,\mathrm{in}}, \quad (11a)$$

$$\frac{dm}{dt} \approx -iG_1 a_1^\dagger. \quad (11b)$$

In the weak-coupling regime $G_1 \ll \kappa_1$, the cavity is damped at a rate that is much faster than the rate at which the magnon mode changes the cavity state, thus the cavity will reach a quasistationary state, which quickly adjusts to changes in the magnon mode. Therefore, the mode a_1 can be adiabatically eliminated by setting $da_1/dt = 0$, and we have

$$a_1 \approx (-i2G_1/\kappa_1)m^\dagger + (2/\sqrt{\kappa_1})a_{1,\mathrm{in}}. \quad (12)$$

The white noise $a_{1,\mathrm{in}}$ has an infinite bandwidth; thus it is not strictly possible to slave a_1 that only responds to a finite bandwidth κ_1 to the vacuum fluctuation. However, as far as the magnon mode m is concerned, vacuum fluctuation restricted to a finite bandwidth can be effectively treated as white noise; hence there is no harm that a_1 is subject to the vacuum fluctuation [58]. Although the noise $a_{1,\mathrm{in}}$ restricted to a finite bandwidth in the adiabatic elimination leads to an incorrect communication relation of a_1, it is known that only the frequency near resonance with the system is important; the high-frequency part of the noise which is far from resonance contributes little when tracing over the bath. Hence the adiabatic elimination of mode a_1 can simplify the calculation while maintaining physical reliability.

Substituting the expression of a_1 into the input-output relation $a_{1,\mathrm{out}} = -a_{1,\mathrm{in}} + \sqrt{\kappa_1}a_1$ and Eq. (11b), we get

$$a_{1,\mathrm{out}} = a_{1,\mathrm{in}} - i\sqrt{2\tilde{G}_1}m^\dagger, \quad (13a)$$

$$\frac{dm}{dt} = \tilde{G}_1 m - i\sqrt{2\tilde{G}_1}a_{1,\mathrm{in}}^\dagger, \quad (13b)$$

where $\tilde{G}_1 = 2{G_1}^2/\kappa_1$. To solve these equations, it is convenient to introduce the effective temporal modes [59,60]. For cavity mode 2 driven by a pulse with the duration $t = \tau_1$, the

effective temporal modes read

$$A_{1,\mathrm{in}}(\tau_1) = \sqrt{\frac{2\tilde{G}_1}{1-e^{-2\tilde{G}_1\tau_1}}}\int_0^{\tau_1} dt\, e^{-\tilde{G}_1 t} a_{1,\mathrm{in}}(t), \quad (14a)$$

$$A_{1,\mathrm{out}}(\tau_1) = \sqrt{\frac{2\tilde{G}_1}{e^{2\tilde{G}_1\tau_1}-1}}\int_0^{\tau_1} dt\, e^{\tilde{G}_1 t} a_{1,\mathrm{out}}(t). \quad (14b)$$

Then the explicit solution of Eq. (13b) can be expressed as

$$m(\tau_1) = e^{\tilde{G}_1\tau_1} m(0) - i\sqrt{e^{2\tilde{G}_1\tau_1}-1} A^\dagger_{1,\mathrm{in}}(\tau_1). \quad (15)$$

Note that Eq. (13b) can be rewritten as $a^\dagger_{1,\mathrm{in}} = (1/i\sqrt{2\tilde{G}_1})(\tilde{G}_1 m - \frac{dm}{dt})$. Substituting that into Eq. (13a), we obtain the equation of motion $\frac{dm}{dt} + \tilde{G}_1 m = -i\sqrt{2\tilde{G}_1} a^\dagger_{1,\mathrm{out}}$, which relates the dynamic evolution of magnons to the output optical field. The solution of this equation is given by $m(\tau_1) = e^{-\tilde{G}_1\tau_1} m(0) - i\sqrt{e^{1-2\tilde{G}_1\tau_1}} A^\dagger_{1,\mathrm{out}}(\tau_1)$. Combining this with Eq. (15), we have

$$A_{1,\mathrm{out}}(\tau_1) = e^{\tilde{G}_1\tau_1} A_{1,\mathrm{in}}(\tau_1) - i\sqrt{e^{2\tilde{G}_1\tau_1}-1} m^\dagger(0). \quad (16)$$

The solutions (15) and (16) can be written as $A_{1,\mathrm{out}} = U_1^\dagger(\tau_1) A_{1,\mathrm{in}} U_1(\tau_1)$ and $m(\tau_1) = U_1^\dagger(\tau_1) m(0) U_1(\tau_1)$, where the propagator $U_1(\tau_1)$ is extracted as [60]

$$U_1(\tau_1) = e^{-i\sqrt{p}A^\dagger_{1,\mathrm{in}} m^\dagger} e^{-\tilde{G}_1\tau_1(1+A^\dagger_{1,\mathrm{in}}A_{1,\mathrm{in}}+m^\dagger m)} e^{i\sqrt{p}A_{1,\mathrm{in}} m}, \quad (17)$$

with $p = 1 - e^{-2\tilde{G}_1\tau_1}$. Assuming that the system is initially in the vacuum state $\rho_0 = |000\rangle_{A_1A_2m}\langle 000|$, at the end of the pumping pulse, the system evolves into

$$\rho_1 = U_1(\tau_1)|000\rangle_{A_1A_2m}\langle 000|U_1^\dagger(\tau_1). \quad (18)$$

Note that the operators $A_{1,\mathrm{in}}m$, $A^\dagger_{1,\mathrm{in}}A_{1,\mathrm{in}}$, and $m^\dagger m$ have zero eigenvalue for the state $|000\rangle$, so $\rho_1 = e^{-2\tilde{G}_1\tau_1} e^{-i\sqrt{p}A^\dagger_{1,\mathrm{in}}m^\dagger}|000\rangle_{A_1A_2m}\langle 000| e^{i\sqrt{p}A_{1,\mathrm{in}}m}$. Then we have

$$\rho_1 = (1-p)\sum_{n,n'=0}^{\infty} (-1)^n (i\sqrt{p})^{n+n'} |n,0,n\rangle_{A_1A_2m}\langle n',0,n'|. \quad (19)$$

It is clear that optical mode 1 and the magnon mode are entangled and optical mode 2 stays in the vacuum state. We introduce formally $p = 1 - e^{-2\tilde{G}_1\tau_1} = \tanh^2 r$ and $1-p = e^{-2\tilde{G}_1\tau_1} = \cosh^{-2} r$, where r denotes the squeezing parameter. Then the state of mode 1 and the magnon mode becomes $|\Psi\rangle_{A_1,m} = \cosh^{-1} r \sum_{n=0}^{\infty}(-i)^n \tanh^n r |n,n\rangle_{A_1,m}$, which is the standard form of the two-mode squeezed state.

In order to test the Bell inequality by using the entanglement between mode 1 and the magnon mode m, the magnonic state should be transferred to optical mode 2 for the measurement purpose. We now consider that cavity mode 1 is pumped by the second pumping pulse. In this case, the dynamics of mode 2 and the magnon mode is described by the Hamiltonian $H_{\mathrm{int}2}$. The corresponding simplified quantum Langevin equations are

$$\frac{da_2}{dt} \approx -iG_2 m - \frac{\kappa_2}{2} a_2 + \sqrt{\kappa_2} a_{2,\mathrm{in}}, \quad (20a)$$

$$\frac{dm}{dt} \approx -iG_2 a_2. \quad (20b)$$

Following the same procedures as discussed for mode 1 and the magnon mode, we can obtain $a_{2,\mathrm{out}} = a_{2,\mathrm{in}} - i\sqrt{2\tilde{G}_2} m$ and $\frac{dm}{dt} = -\tilde{G}_2 m - i\sqrt{2\tilde{G}_2} a_{1,\mathrm{in}}$, where $\tilde{G}_2 = 2{G_2}^2/\kappa_2$. By introducing the effective temporal modes of cavity mode 2,

$$A_{2,\mathrm{in}}(\tau_2) = \sqrt{\frac{2\tilde{G}_2}{e^{2\tilde{G}_2\tau_2}-1}}\int_0^{\tau_2} dt\, e^{\tilde{G}_2 t} a_{2,\mathrm{in}}(t), \quad (21a)$$

$$A_{2,\mathrm{out}}(\tau_2) = \sqrt{\frac{2\tilde{G}_2}{1-e^{-2\tilde{G}_2\tau_2}}}\int_0^{\tau_2} dt\, e^{-\tilde{G}_2 t} a_{2,\mathrm{out}}(t), \quad (21b)$$

with the duration τ_2 of the pumping pulse, we have

$$A_{2,\mathrm{out}}(\tau_2) = e^{-\tilde{G}_2\tau_2} A_{2,\mathrm{in}}(\tau_2) - i\sqrt{1-e^{-2\tilde{G}_2\tau_2}} m(0), \quad (22a)$$

$$m(\tau_2) = e^{-\tilde{G}_2\tau_2} m(0) - i\sqrt{1-e^{-2\tilde{G}_2\tau_2}} A_{2,\mathrm{in}}(\tau_2). \quad (22b)$$

By rewriting the solutions (22a) and (22b) as $A_{2,\mathrm{out}} = U_2^\dagger(\tau_2) A_{2,\mathrm{in}} U_2(\tau_2)$ and $m(\tau_2) = U_2^\dagger(\tau_2) m(0) U_2(\tau_2)$, the propagator $U_2(\tau_2)$ can be obtained as

$$U_2(\tau_2) = e^{-i\sqrt{T'}A^\dagger_{2,\mathrm{in}}m} e^{\tilde{G}_2\tau_2(A^\dagger_{2,\mathrm{in}}A_{2,\mathrm{in}}-m^\dagger m)} e^{i\sqrt{T'}A_{2,\mathrm{in}}m^\dagger}, \quad (23)$$

with $T' = e^{2\tilde{G}_2\tau_2} T$, where $T = 1 - e^{-2\tilde{G}_2\tau_2}$ defines the conversion efficiency between the magnon mode m and mode 2. If $\tilde{G}_2\tau_2$ is sufficiently large, Eq. (22a) is reduced to $A_{2,\mathrm{out}}(\tau_2) = -im(0)$. This means that the magnon quantum state created by the first pulse can be nearly perfectly mapped onto optical mode 2 apart from a phase shift. When the two cavity modes and the magnon mode are initially in the vacuum state, by sequentially pumping the two cavity modes at resonance, the final state of the system can be described by the density matrix

$$\rho_2 = U_2(\tau_2) U_1(\tau_1)|000\rangle_{A_1A_2m}\langle 000|U_1^\dagger(\tau_1) U_2^\dagger(\tau_2). \quad (24)$$

Recalling Eqs. (18) and (19), the density matrix can be written as $\rho_2 = U_2(\tau_2)\rho_1 U_2^\dagger(\tau_2)$. Then the density matrix is calculated as

$$\rho_2 = (1-p)\sum_{n,n'=0}^{\infty} (-\sqrt{pT})^{n+n'} |n,n,0\rangle_{A_1A_2m}\langle n',n',0|. \quad (25)$$

By tracing out the magnon mode, we gain the density matrix of the two traveling optical pulses

$$\rho_{A_1A_2} = (1-p)\sum_{n=0}^{\infty} (-\sqrt{pT})^{n+n'} |n,n\rangle_{A_1A_2}\langle n',n'|. \quad (26)$$

In the case of $\tilde{G}_2\tau_2 \gg 1$, the conversion efficiency T approaches 1 and the state $\rho_{A_1A_2}$ is close to the two-mode squeezed state.

B. Violation of the CHSH inequality

The type of Bell inequality relevant to our proposal is the CHSH inequality [42]. We are interested in the measurements that allow us to identify the vacuum state and all nonzero-photon-number states, i.e., the on-off detection. When the application of coherent displacement $D(\alpha)$ is in front of the photon detector, the measurement can be described by the positive-operator-valued measure with two orthogonal projection operators $P_\alpha = D(\alpha)|0\rangle\langle 0|D^\dagger(\alpha) = |\alpha\rangle\langle\alpha|$ and $Q_\alpha = \mathbb{I} - |\alpha\rangle\langle\alpha|$. We assign the outcome $+1$ to the detection of

$|\alpha\rangle$ and -1 otherwise; then the observable for the system is described by $2P_\alpha - \mathbb{I}$. Therefore, the correlation function $E_{\alpha\beta} = \langle(2P_\alpha - \mathbb{I}) \otimes (2P_\beta - \mathbb{I})\rangle$ for the two optical fields is given by

$$E_{\alpha\beta} = 4P(+1+1|\alpha\beta) - 2[P(+1|\alpha) + P(+1|\beta)] + 1. \tag{27}$$

Here $P(+1+1|\alpha\beta) = \langle P_\alpha \otimes P_\beta\rangle$ represents the joint probability to get the measurement outcome $+1$ for both optical fields, and $P(+1|\alpha) = \langle P_\alpha \otimes \mathbb{I}\rangle$ and $P(+1|\beta) = \langle \mathbb{I} \otimes P_\beta\rangle$ are the probabilities of measuring a single field with outcome $+1$. The observable and correlation of such a form for Bell tests were introduced in Refs. [61–64] and had been realized in experiments with optical two-mode squeezed states produced by spontaneous parametric down-conversion [57].

For the local hidden-variable model, the four correlation functions between pairs of measurements obey the CHSH inequality

$$S = |E_{\alpha_1\beta_1} + E_{\alpha_1\beta_2} + E_{\alpha_2\beta_1} - E_{\alpha_2\beta_2}| \leqslant 2. \tag{28}$$

The inequality can be violated with a proper choice of the observables measured on the quantum entanglement states, and the allowed maximal violation is $S = 2\sqrt{2}$ [41]. We now proceed to discuss the correlation function $E_{\alpha\beta}$ between optical modes 1 and 2. The joint probability of measurement outcomes $+1$ for both modes 1 and 2 can be written as $P(+1+1|\alpha\beta) = \mathrm{Tr}(\rho_{A_1A_2} P_\alpha \otimes P_\beta)$. By using the density matrix given by Eq. (26), we calculate the joint probability as

$$P(+1+1|\alpha\beta) = (1-p)e^{-|\alpha|^2-|\beta|^2} e^{-\sqrt{pT}(\alpha^*\beta^*+\alpha\beta)}. \tag{29}$$

The marginals $P(+1|\alpha) = \mathrm{Tr}(\rho_{A_1A_2} P_\alpha \otimes \mathbb{I})$ and $P(+1|\beta) = \mathrm{Tr}(\rho_{A_1A_2} \mathbb{I} \otimes P_\beta)$ are also given by

$$P(+1|\alpha) = (1-p)e^{-(1-pT)|\alpha|^2} \tag{30}$$

and

$$P(+1|\beta) = (1-p)e^{-(1-pT)|\beta|^2}, \tag{31}$$

respectively. Together with the definition of the correlation function $E_{\alpha\beta}$, the quantity S can be evaluated by Eq. (28).

We optimize the value of S over the measurement settings $\alpha_{1,2}$ and $\beta_{1,2}$, and the results as a function of $\tilde{G}_1\tau_1$ for different conversion efficiencies T are shown in Fig. 2. Obviously, the violation of the CHSH inequality can be obtained with a proper choice of $\tilde{G}_1\tau_1$ and a high conversion efficiency T. The maximal violation $S \approx 2.45$ is achieved at $\tilde{G}_1\tau_1 \approx 0.25$ ($p \approx 0.39$) and $T = 1$. This result agrees well with previous studies [65,66], where the maximal violation of $S \approx 2.45$ for the squeezing parameter $r \approx 0.76$ ($p = \tanh^2 r \approx 0.40$) was obtained for an ideal two-mode squeezed state.

The quantity S versus $\tilde{G}_2\tau_2$ for different values of p is depicted in Fig. 3. It is shown that a significant violation is achieved at $p = 0.39$ with larger $\tilde{G}_2\tau_2$. An efficient conversion requires stronger coupling strength G_2 between the magnon mode and cavity mode 2, which can be obtained by increasing the input pumping power encoded in α_1.

Recall the approximations that have been made in the model: (i) weak-coupling conditions $G_{1,2} \ll \kappa$ and (ii) negligible magnon dissipation, which implies that the pulse duration should be shorter than the magnon decoherence time

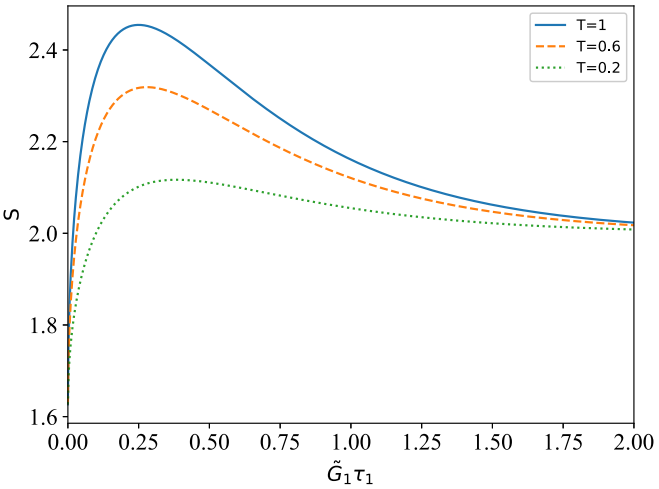

FIG. 2. Optimal values of S as a function of $\tilde{G}_1\tau_1$ for various magnon-photon conversion efficiencies T.

$\tau_1 + \tau_2 \ll (\gamma\bar{n}_{\mathrm{th}})^{-1}$. In the YIG-based cavity optomagnonical system, the cavity decay rate $\kappa \sim 1$ GHz and magnon decay rate $\gamma \sim 1$ MHz were demonstrated in experiment [24,25]. Assuming that the coupling strengths are $G_1 \sim 20$ MHz and $G_2 \sim 100$ MHz, with the pulse durations $\tau_1 \sim 31$ ns and $\tau_2 \sim 75$ ns, an optimal value of $\tilde{G}_1\tau_1$ around 0.25 and high conversion efficiency $T = 1 - e^{-2\tilde{G}_2\tau_2} \approx 0.95$ can be achieved. In this case, the requirement imposed by the two approximations above can be satisfied. Although the required coupling strength is still unavailable in current experiments, great effort has been made to enhance the optomagnonic coupling by reducing the mode volume of the optical mode in the YIG disk [31] or by selecting magnon modes to maximize the overlap of the magnon and photon modes [34]. The coupling strength is expected to be improved in the next-generation experiments.

C. Bell test in phase space

In above discussion we have neglected the influence on measurement of the efficiency of the photon detector and

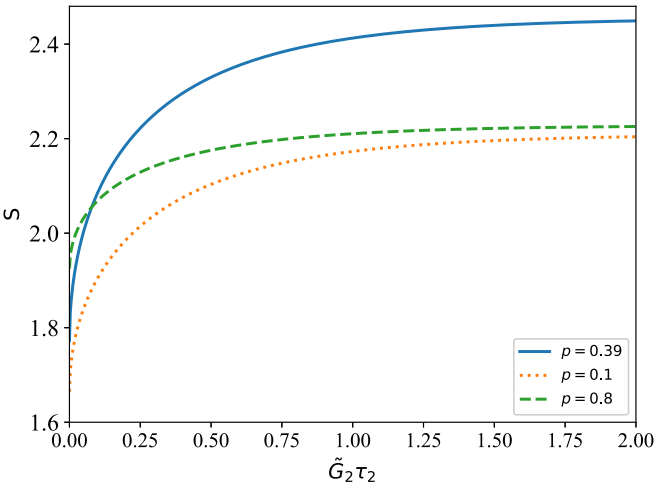

FIG. 3. Optimal values of S as a function of $\tilde{G}_2\tau_2$ for various values of p.

the transmissivity in the beam splitter. In the following, we discuss the proposal for a Bell test including the detector efficiencies in phase space. For the measurement setting in our proposal, it has been shown that the Bell inequality can be studied in the phase space based on the Wigner function or Q function [62]. For the on-off detection, which measures the correlation between the vacuum state and all nonzero-photon-number states, the mean value of the measurement is proportional to the Q functions with $Q(\alpha,\beta)=\frac{1}{\pi^2}P(+1+1|\alpha\beta)$ and $Q(\alpha)=\frac{1}{\pi}P(+1|\alpha)$. The CHSH inequality can be formulated in terms of the Q functions as [62,67]

$$S=\ |4\pi^2[Q(\alpha_1,\beta_1)+Q(\alpha_1,\beta_2)+Q(\alpha_2,\beta_1)-Q(\alpha_2,\beta_2)] -4\pi[Q(\alpha_1)+Q(\beta_1)]+2|\leqslant 2. \tag{32}$$

When the detector efficiency η_d and the transmissivity λ_t of the beam splitter are considered, we follow Ref. [65] and define the overall detection efficiency $\eta=\eta_d\lambda_t$. Thus the CHSH inequality written as a function of η becomes [65]

$$S=\left|\frac{4\pi^2}{\eta^2}[Q_\eta(\alpha_1,\beta_1)+Q_\eta(\alpha_1,\beta_2)+Q_\eta(\alpha_2,\beta_1) -Q_\eta(\alpha_2,\beta_2)]-\frac{4\pi}{\eta}[Q_\eta(\alpha_1)+Q_\eta(\beta_1)]+2\right|\leqslant 2, \tag{33}$$

where the two-mode Q function of the state described in Eq. (26) is given by

$$Q_\eta(\alpha,\beta)=\frac{4}{\pi^2R(\eta)}\exp\left(-2\frac{S(\eta)}{R(\eta)}(|\alpha|^2+|\beta|^2)\right) \times\exp\left(\frac{-4\sqrt{p}}{R(\eta)(1-p)}(\alpha^*\beta^*+\alpha\beta)\right) \tag{34}$$

and the single-mode Q function is

$$Q_\eta(\alpha)=\frac{2}{\pi S(\eta)}\exp\left(-\frac{2}{S(\eta)}|\alpha|^2\right), \tag{35}$$

with $R(\eta)=(1-2/\eta)^2-2(1-2/\eta)(1+p)/(1-p)+1$ and $S(\eta)=(1+p)/(1-p)+2/\eta-1$. Here we have assumed the conversion efficiency $T=1$ for simplicity.

Figure 4 shows S as a function of $\tilde{G}_1\tau_1$ and η at the optimal values of $\alpha_{1,2}$ and $\beta_{1,2}$. Clearly, the violation of the Bell inequality requires a detector efficiency η larger than 0.8. As expected, the maximal violation can be obtained at $\eta=1$ and $\tilde{G}_1\tau_1\approx 0.25$. A high overall detection efficiency can be achieved by the beam splitter with high transmissivity and by the photon detector with small dark count probability.

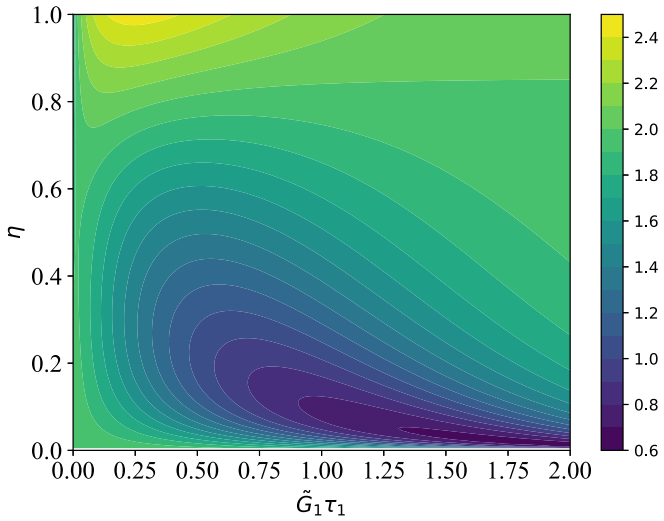

FIG. 4. Contour plot of S versus $\tilde{G}_1\tau_1$ and η for the optimal values of $\alpha_{1,2}$ and $\beta_{1,2}$.

IV. CONCLUSION

We have assumed the weak-coupling condition $G_{1,2}\ll\kappa$ and have neglected the magnon mode decay γ in our model. In our YIG-based cavity optomagnonical system, the intrinsic magnon-photon coupling strength was demonstrated as $g=10.4$ Hz; the effective coupling strength was obtained as $G=g\alpha=73$ kHz with 30 μW optical power and it could be further enhanced to $G=10$ MHz [24]. The weak-coupling condition $G_{1,2}\ll\kappa$ corresponds to the experimental parameters. However, in order to reasonably neglect the decay of the magnon mode, the pulse duration should be shorter than the magnon decoherence time, which in turn requires a stronger coupling strength to obtain the optimal values of $\tilde{G}_1\tau_1$ and $\tilde{G}_2\tau_2$. Although the required coupling strength is not available in the optomagnonic system, it is expected that the coupling strength will be improved in future experiments. In addition, we have assumed for simplicity that the magnon mode is initially prepared in its ground state. Indeed, a rigorous proposal should include the case that the magnon mode is initially in a thermal state. For a YIG sphere with magnon frequency $\omega_m=7.95$ GHz, the average thermal magnon number in a dilution refrigerator at temperature 10 mK is $n_0=0.026$ [18]. For such a small average thermal magnon number, it may not seriously affect the violation of the Bell inequality [53,54].

In summary, we have proposed a scheme to implement the violation of the Bell inequality in cavity optomagnonics, where a magnon mode couples with two nondegenerate cavity modes. Our model corresponds to recent YIG-based experiments and takes into account the selection rules of angular momentum and the triple-resonance condition. The Langevin equations of the optomagnonical system were solved and the experimental implementation of the Bell test was analyzed in detail. The results show that a significant violation of the Bell inequality can be achieved by a proper choice of $\tilde{G}_1\tau_1$, high magnon-photon conversion efficiency T, and high overall detection efficiency η.

ACKNOWLEDGMENTS

We acknowledge support from the National Natural Science Foundation of China (Grants No. 12174054, No. 12074067, No. 11847056, No. 12004336, and No. 11674059) and the Natural Science Foundation of Fujian Province of China (Grants No. 2021J011228, No. 2020J01191, and No. 2019J01431).

[1] L.-M. Duan, M. D. Lukin, J. I. Cirac, and P. Zoller, Long-distance quantum communication with atomic ensembles and linear optics, Nature (London) **414**, 413 (2001).

[2] H. J. Kimble, The quantum internet, Nature (London) **453**, 1023 (2008).

[3] S. Wehner, D. Elkouss, and R. Hanson, Quantum internet: A vision for the road ahead, Science **362**, eaam9288 (2018).

[4] C. L. Degen, F. Reinhard, and P. Cappellaro, Quantum sensing, Rev. Mod. Phys. **89**, 035002 (2017).

[5] D. Lachance-Quirion, Y. Tabuchi, A. Gloppe, K. Usami, and Y. Nakamura, Hybrid quantum systems based on magnonics, Appl. Phys. Express **12**, 070101 (2019).

[6] B. Z. Rameshti, S. V. Kusminskiy, J. A. Haigh, K. Usami, D. Lachance-Quirion, Y. Nakamura, C.-M. Hu, H. X. Tang, G. E. Bauer, and Y. M. Blanter, Cavity magnonics, arXiv:2106.09312.

[7] O. O. Soykal and M. E. Flatté, Strong Field Interactions between a Nanomagnet and a Photonic Cavity, Phys. Rev. Lett. **104**, 077202 (2010).

[8] H. Huebl, C. W. Zollitsch, J. Lotze, F. Hocke, M. Greifenstein, A. Marx, R. Gross, and S. T. B. Goennenwein, High Cooperativity in Coupled Microwave Resonator Ferrimagnetic Insulator Hybrids, Phys. Rev. Lett. **111**, 127003 (2013).

[9] Y. Tabuchi, S. Ishino, T. Ishikawa, R. Yamazaki, K. Usami, and Y. Nakamura, Hybridizing Ferromagnetic Magnons and Microwave Photons in the Quantum Limit, Phys. Rev. Lett. **113**, 083603 (2014).

[10] X. Zhang, C.-L. Zou, L. Jiang, and H. X. Tang, Strongly Coupled Magnons and Cavity Microwave Photons, Phys. Rev. Lett. **113**, 156401 (2014).

[11] M. Goryachev, W. G. Farr, D. L. Creedon, Y. Fan, M. Kostylev, and M. E. Tobar, High-Cooperativity Cavity QED with Magnons at Microwave Frequencies, Phys. Rev. Appl. **2**, 054002 (2014).

[12] Y.-P. Wang, G.-Q. Zhang, D. Zhang, T.-F. Li, C.-M. Hu, and J. Q. You, Bistability of Cavity Magnon Polaritons, Phys. Rev. Lett. **120**, 057202 (2018).

[13] J. T. Hou and L. Liu, Strong Coupling between Microwave Photons and Nanomagnet Magnons, Phys. Rev. Lett. **123**, 107702 (2019).

[14] Y. Li, T. Polakovic, Y.-L. Wang, J. Xu, S. Lendinez, Z. Zhang, J. Ding, T. Khaire, H. Saglam, R. Divan, J. Pearson, W.-K. Kwok, Z. Xiao, V. Novosad, A. Hoffmann, and W. Zhang, Strong Coupling between Magnons and Microwave Photons in On-Chip Ferromagnet-Superconductor Thin-Film Devices, Phys. Rev. Lett. **123**, 107701 (2019).

[15] H. Y. Yuan, P. Yan, S. Zheng, Q. Y. He, K. Xia, and M.-H. Yung, Steady Bell State Generation via Magnon-Photon Coupling, Phys. Rev. Lett. **124**, 053602 (2020).

[16] H. Y. Yuan, S. Zheng, Z. Ficek, Q. Y. He, and M.-H. Yung, Enhancement of magnon-magnon entanglement inside a cavity, Phys. Rev. B **101**, 014419 (2020).

[17] Y. Tabuchi, S. Ishino, A. Noguchi, T. Ishikawa, R. Yamazaki, K. Usami, and Y. Nakamura, Coherent coupling between a ferromagnetic magnon and a superconducting qubit, Science **349**, 405 (2015).

[18] D. Lachance-Quirion, Y. Tabuchi, S. Ishino, A. Noguchi, T. Ishikawa, R. Yamazaki, and Y. Nakamura, Resolving quanta of collective spin excitations in a millimeter-sized ferromagnet, Sci. Adv. **3**, e1603150 (2017).

[19] X. Zhang, C.-L. Zou, L. Jiang, and H. X. Tang, Cavity magnomechanics, Sci. Adv. **2**, e1501286 (2016).

[20] J. Li, S.-Y. Zhu, and G. S. Agarwal, Magnon-Photon-Phonon Entanglement in Cavity Magnomechanics, Phys. Rev. Lett. **121**, 203601 (2018).

[21] S. Viola Kusminskiy, in *Optomagnonic Structures: Novel Architectures for Simultaneous Control of Light and Spin Waves*, edited by E. Almpanis (World Scientific, Singapore, 2021), pp. 299–353.

[22] R. Hisatomi, A. Osada, Y. Tabuchi, T. Ishikawa, A. Noguchi, R. Yamazaki, K. Usami, and Y. Nakamura, Bidirectional conversion between microwave and light via ferromagnetic magnons, Phys. Rev. B **93**, 174427 (2016).

[23] A. Osada, R. Hisatomi, A. Noguchi, Y. Tabuchi, R. Yamazaki, K. Usami, M. Sadgrove, R. Yalla, M. Nomura, and Y. Nakamura, Cavity Optomagnonics with Spin-Orbit Coupled Photons, Phys. Rev. Lett. **116**, 223601 (2016).

[24] X. Zhang, N. Zhu, C.-L. Zou, and H. X. Tang, Optomagnonic Whispering Gallery Microresonators, Phys. Rev. Lett. **117**, 123605 (2016).

[25] J. A. Haigh, A. Nunnenkamp, A. J. Ramsay, and A. J. Ferguson, Triple-Resonant Brillouin Light Scattering in Magneto-Optical Cavities, Phys. Rev. Lett. **117**, 133602 (2016).

[26] A. Osada, A. Gloppe, R. Hisatomi, A. Noguchi, R. Yamazaki, M. Nomura, Y. Nakamura, and K. Usami, Brillouin Light Scattering by Magnetic Quasivortices in Cavity Optomagnonics, Phys. Rev. Lett. **120**, 133602 (2018).

[27] R. Hisatomi, A. Noguchi, R. Yamazaki, Y. Nakata, A. Gloppe, Y. Nakamura, and K. Usami, Helicity-Changing Brillouin Light Scattering by Magnons in a Ferromagnetic Crystal, Phys. Rev. Lett. **123**, 207401 (2019).

[28] T. Liu, X. Zhang, H. X. Tang, and M. E. Flatté, Optomagnonics in magnetic solids, Phys. Rev. B **94**, 060405(R) (2016).

[29] S. Viola Kusminskiy, H. X. Tang, and F. Marquardt, Coupled spin-light dynamics in cavity optomagnonics, Phys. Rev. A **94**, 033821 (2016).

[30] S. Sharma, Y. M. Blanter, and G. E. W. Bauer, Light scattering by magnons in whispering gallery mode cavities, Phys. Rev. B **96**, 094412 (2017).

[31] J. Graf, H. Pfeifer, F. Marquardt, and S. Viola Kusminskiy, Cavity optomagnonics with magnetic textures: Coupling a magnetic vortex to light, Phys. Rev. B **98**, 241406(R) (2018).

[32] A. Osada, A. Gloppe, Y. Nakamura, and K. Usami, Orbital angular momentum conservation in Brillouin light scattering within a ferromagnetic sphere, New J. Phys. **20**, 103018 (2018).

[33] J. A. Haigh, N. J. Lambert, S. Sharma, Y. M. Blanter, G. E. W. Bauer, and A. J. Ramsay, Selection rules for cavity-enhanced Brillouin light scattering from magnetostatic modes, Phys. Rev. B **97**, 214423 (2018).

[34] S. Sharma, B. Z. Rameshti, Y. M. Blanter, and G. E. W. Bauer, Optimal mode matching in cavity optomagnonics, Phys. Rev. B **99**, 214423 (2019).

[35] W.-J. Wu, Y.-P. Wang, J.-Z. Wu, J. Li, and J. Q. You, Remote magnon entanglement between two massive ferrimagnetic spheres via cavity optomagnonics, Phys. Rev. A **104**, 023711 (2021).

[36] S. Sharma, Y. M. Blanter, and G. E. W. Bauer, Optical Cooling of Magnons, Phys. Rev. Lett. **121**, 087205 (2018).

[37] V. A. S. V. Bittencourt, V. Feulner, and S. V. Kusminskiy, Magnon heralding in cavity optomagnonics, Phys. Rev. A **100**, 013810 (2019).

[38] Y.-P. Gao, X.-F. Liu, T.-J. Wang, C. Cao, and C. Wang, Photon excitation and photon-blockade effects in optomagnonic microcavities, Phys. Rev. A **100**, 043831 (2019).

[39] S. Sharma, V. A. S. V. Bittencourt, A. D. Karenowska, and S. V. Kusminskiy, Spin cat states in ferromagnetic insulators, Phys. Rev. B **103**, L100403 (2021).

[40] F.-X. Sun, S.-S. Zheng, Y. Xiao, Q. Gong, Q. He, and K. Xia, Remote Generation of Magnon Schrödinger Cat State via Magnon-Photon Entanglement, Phys. Rev. Lett. **127**, 087203 (2021).

[41] N. Brunner, D. Cavalcanti, S. Pironio, V. Scarani, and S. Wehner, Bell nonlocality, Rev. Mod. Phys. **86**, 419 (2014).

[42] J. F. Clauser, M. A. Horne, A. Shimony, and R. A. Holt, Proposed Experiment to Test Local Hidden-Variable Theories, Phys. Rev. Lett. **23**, 880 (1969).

[43] S. J. Freedman and J. F. Clauser, Experimental Test of Local Hidden-Variable Theories, Phys. Rev. Lett. **28**, 938 (1972).

[44] A. Aspect, P. Grangier, and G. Roger, Experimental Tests of Realistic Local Theories via Bell's Theorem, Phys. Rev. Lett. **47**, 460 (1981).

[45] Y. H. Shih and C. O. Alley, New Type of Einstein-Podolsky-Rosen-Bohm Experiment using Pairs of Light Quanta Produced by Optical Parametric Down Conversion, Phys. Rev. Lett. **61**, 2921 (1988).

[46] J. G. Rarity and P. R. Tapster, Experimental Violation of Bell's Inequality Based on Phase and Momentum, Phys. Rev. Lett. **64**, 2495 (1990).

[47] P. G. Kwiat, K. Mattle, H. Weinfurter, A. Zeilinger, A. V. Sergienko, and Y. Shih, New High-Intensity Source of Polarization-Entangled Photon Pairs, Phys. Rev. Lett. **75**, 4337 (1995).

[48] G. Weihs, T. Jennewein, C. Simon, H. Weinfurter, and A. Zeilinger, Violation of Bell's Inequality under Strict Einstein Locality Conditions, Phys. Rev. Lett. **81**, 5039 (1998).

[49] M. A. Rowe, D. Kielpinski, V. Meyer, C. A. Sackett, W. M. Itano, C. Monroe, and D. J. Wineland, Experimental violation of a Bell's inequality with efficient detection, Nature (London) **409**, 791 (2001).

[50] B. Hensen, H. Bernien, A. E. Dréau, A. Reiserer, N. Kalb, M. S. Blok, J. Ruitenberg, R. F. Vermeulen, R. N. Schouten, C. Abellán *et al.*, Loophole-free Bell inequality violation using electron spins separated by 1.3 kilometres, Nature (London) **526**, 682 (2015).

[51] M. Giustina, M. A. M. Versteegh, S. Wengerowsky, J. Handsteiner, A. Hochrainer, K. Phelan, F. Steinlechner, J. Kofler, J.-A. Larsson, C. Abellán, W. Amaya, V. Pruneri, M. W. Mitchell, J. Beyer, T. Gerrits, A. E. Lita, L. K. Shalm, S. W. Nam, T. Scheidl, R. Ursin *et al.*, Significant-Loophole-Free Test of Bell's Theorem with Entangled Photons, Phys. Rev. Lett. **115**, 250401 (2015).

[52] L. K. Shalm, E. Meyer-Scott, B. G. Christensen, P. Bierhorst, M. A. Wayne, M. J. Stevens, T. Gerrits, S. Glancy, D. R. Hamel, M. S. Allman *et al.*, Strong Loophole-Free Test of Local Realism, Phys. Rev. Lett. **115**, 250402 (2015).

[53] V. C. Vivoli, T. Barnea, C. Galland, and N. Sangouard, Proposal for an Optomechanical Bell Test, Phys. Rev. Lett. **116**, 070405 (2016).

[54] S. G. Hofer, K. W. Lehnert, and K. Hammerer, Proposal to Test Bell's Inequality in Electromechanics, Phys. Rev. Lett. **116**, 070406 (2016).

[55] I. Marinković, A. Wallucks, R. Riedinger, S. Hong, M. Aspelmeyer, and S. Gröblacher, Optomechanical Bell Test, Phys. Rev. Lett. **121**, 220404 (2018).

[56] M. G. A. Paris, Displacement operator by beam splitter, Phys. Lett. A **217**, 78 (1996).

[57] A. Kuzmich, I. A. Walmsley, and L. Mandel, Violation of Bell's Inequality by a Generalized Einstein-Podolsky-Rosen State using Homodyne Detection, Phys. Rev. Lett. **85**, 1349 (2000).

[58] H. M. Wiseman and G. J. Milburn, All-optical versus electro-optical quantum-limited feedback, Phys. Rev. A **49**, 4110 (1994).

[59] S. G. Hofer, W. Wieczorek, M. Aspelmeyer, and K. Hammerer, Quantum entanglement and teleportation in pulsed cavity optomechanics, Phys. Rev. A **84**, 052327 (2011).

[60] C. Galland, N. Sangouard, N. Piro, N. Gisin, and T. J. Kippenberg, Heralded Single-Phonon Preparation, Storage, and Readout in Cavity Optomechanics, Phys. Rev. Lett. **112**, 143602 (2014).

[61] S. M. Tan, D. F. Walls, and M. J. Collett, Nonlocality of a Single Photon, Phys. Rev. Lett. **66**, 252 (1991).

[62] K. Banaszek and K. Wódkiewicz, Testing Quantum Nonlocality in Phase Space, Phys. Rev. Lett. **82**, 2009 (1999).

[63] L. Hardy, Nonlocality of a Single Photon Revisited, Phys. Rev. Lett. **73**, 2279 (1994).

[64] B. Hessmo, P. Usachev, H. Heydari, and G. Björk, Experimental Demonstration of Single Photon Nonlocality, Phys. Rev. Lett. **92**, 180401 (2004).

[65] S.-W. Lee, H. Jeong, and D. Jaksch, Testing quantum nonlocality by generalized quasiprobability functions, Phys. Rev. A **80**, 022104 (2009).

[66] J. B. Brask and R. Chaves, Robust nonlocality tests with displacement-based measurements, Phys. Rev. A **86**, 010103(R) (2012).

[67] J. Li and S.-Y. Zhu, Einstein-Podolsky-Rosen steering and Bell nonlocality of two macroscopic mechanical oscillators in optomechanical systems, Phys. Rev. A **96**, 062115 (2017).